



CHEMICAL SCIENCES

Photocatalytic performance of SiO₂@TiO₂ spheres in selective conversion of oxidation of benzyl alcohol to benzaldehyde and reduction of nitrobenzene to aniline

BRUNO C.B. SALGADO & ANTONINHO VALENTINI

Abstract: Selective photocatalytic oxidation of benzyl alcohol to benzaldehyde and reduction of nitrobenzene to aniline reactions are investigated by using SiO₂@TiO₂ spheres produced in a simple route using chitosan as a template. The spheres are predominantly macroporous and, the XRD points out an amorphous crystallographic profile suggesting the uniform distribution of TiO₂. Under low-power lighting for 4 hours, the conversions achieved was of the order of 49% and 99% for benzyl alcohol and nitrobenzene, respectively, with selectivity to benzaldehyde and aniline of 99% in both reactions. The study also follows the effects of the solvent and the presence of O₂.

Key words: Selective photocatalysis, silica sphere, titania.

INTRODUCTION

Heterogeneous photocatalysis is an alternative method for decomposing organic contaminants. In this sense, it is found several works which explore the photocatalytic process to decompose water pollutants, such as pesticides (Affam & Chaudhuri 2013, Berberidou et al. 2017, Gomes Júnior et al. 2017), dyes (Colpini et al. 2014, Marugán et al. 2007, Salehi et al. 2012, Wang et al. 2019a), aromatic hydrocarbons (Bai et al. 2017, Gao et al. 2020, Monteagudo et al. 2020, Vela et al. 2012, Zhang et al. 2008), pharmaceutical waste (Finčur et al. 2017, Gao et al. 2020, Molinari et al. 2017, Salaeh et al. 2016, Serna-Galvis et al. 2016), polychlorinated and polybrominated biphenyls (Shaban et al. 2016, Wang et al. 2019b, Zhu et al. 2016) and other organic compounds (Kumari et al. 2020).

However, the photocatalytic process can promote reduction or oxidation reactions with good selectivity (Imamura et al. 2013). Additionally, it is worth mentioning that the photocatalytic process needs mild temperature and pressure conditions (Fukui et al. 2019, Livingstone et al. 2019). This versatility contributes to the development of new studies that have led to the improvement of the photocatalytic technique as an innovative method in the field of fine chemistry, even enabling the use of renewable resources (solar radiation and biomass) as an energy source for the propagation of the phenomenon.

On the other hand, photocatalysis can selectively produce the conversion of the $-\text{CH}_2\text{OH}$ to $-\text{CHO}$ group, enabling the production of compounds from the aldehyde group under mild conditions, which are widely applied as precursors of various medicines, vitamins, and fragrances (Pillai & Sahle-Demessie 2003). The conventional route of aldehyde production contributes to the release of metallic waste derived from the catalysts used, generating negative impacts on the environment (Xie et al. 2014). In the proposed photocatalytic mechanism for this reaction, one step is the reaction of the alcoholic substrate with the photogenerated positive holes (h_{VB}^+) and the molecular oxygen (O_2) acts as a photoelectrons acceptor (Turchi 1990). The photocatalytic oxidation selectivity is higher by using an organic solvent, such as acetonitrile. Using water produces hydroxyl radical, highly reactive (Spasiano et al. 2013). The O_2 , however, can generate the superoxide radical, hydrogen peroxide, and hydroxyl radical (Nosaka & Nosaka 2017). Therefore, to improve the photocatalytic selectivity, it would be interesting to use another photoelectron acceptor.

Aniline is a compound widely used to produce pharmaceuticals, dyes, pigments, and pesticides in laboratory and industrial scales (Corma et al. 2007, Wang et al. 2010). As with benzaldehyde, the industrial production route involves the release of waste containing metallic catalysts harmful to the environment. Furthermore, the traditional catalytic process (Ni, Pt, or Pd under H_2 pressure) leads to the hydrogenation of the phenyl group, resulting in a low selectivity (Shiraishi et al. 2012). Alternatively, photocatalysis can promote this reaction, which means to be possible to introduce a method with lower residues production. Therefore, the nitrobenzene reduction to aniline is an interesting process to act as a photoelectron acceptor.

Although both processes, the benzaldehyde and the aniline production, have been known for a long time (Buck et al. 1987, Lawrence 1983, Spiegler & Graham 1958), industrially a large amount of waste is still produced. These wastes require treatment, but sometimes they are often just stored, subject to possible environmental accidents. Thus, it is necessary to implement a production process for such products or their derivatives, which generates a lower amount of waste.

The need to decrease the environmental impact has encouraged research, either to explore the reaction or to test the photocatalytic activity of new materials for H_2 evolution or oxidation of organic pollutants (Fiorenza et al. 2019, Tahir & Tahir 2020, Wojtyła et al. 2020). But the low cost, no toxicity, and high oxidizing activity are properties that make the TiO_2 be widely used for photocatalytic process (Chen et al. 2010, Colmenares et al. 2016, Flores et al. 2007, Huang et al. 2010, Kominami et al. 2009, Palmisano et al. 2007b 2006, Shiraishi et al. 2012, Zhang et al. 2009).

Generally, the TiO_2 is prepared as finely particulate material, which difficult the recovery for reusing (Horikoshi & Serpone 2020). To make more accessible the recovering process, the TiO_2 can alternatively be prepared as a supported catalyst (Fiorenza et al. 2019, Ho et al. 2019, Islam et al. 2020). With this goal in mind, numerous solid matrices have been used as support material for the active phase (Islam et al. 2020). But, SiO_2 has been pointed out as the most interesting support because it is chemically inert, transparent to UV radiation, and has a high surface area (Bellardita et al. 2010, Gude et al. 2008). Porous materials with a high surface area tend to increase the rate and amount of substrate adsorption, enhancing the TiO_2 performance of superficially exposed contact with the adsorbate.

Parallel to the supporting process, the pellet shape and diameter also can affect the catalytic performance. The synthesis route of macroporous spheres of SiO_2 or Al_2O_3 presented previously

(Braga et al. 2009, Santos et al. 2015) may produce a sample with a spherical shape and diameter near 1.0 μm and easy separation process. Additionally, spheres with such a diameter range are easily kept in suspension in the reaction solution, either under the gas flow or under the solution flow itself.

The photocatalytic macroporous sphere was synthesized (SiO₂ spheres with a diameter near 1.0 μm containing TiO₂) by the method presented previously (Braga et al. 2009), aiming to explore the synthesis route. Additionally, with the aim to contribute to a lower reaction by-product formation, the sample was tested for the photocatalytic performance for benzyl alcohol oxidation and the nitrobenzene reduction reactions.

MATERIALS AND METHODS

Preparation of the SiO₂@TiO₂ spheres

The SiO₂ spheres were synthesized using the hybrid system, SiO₂ precursors, and chitosan (Braga et al. 2009). Under continuous stirring, the chitosan (CTS) (3% m/v) was dispersed in an aqueous solution of acetic acid (5% v/v). Following, equimolar amounts of particulate SiO₂ (Aerosil, Degussa Evonik) and tetraethylorthosilicate (TEOS, Aldrich) were added in the same solution, yielding a molar ratio of 1:1.5 between CTS monomer to Si. This mixture was dripped in an alkaline medium (NH₄OH, 30%) using a peristaltic pump. The formed spheres were removed and dried at room temperature for 72 hours. The hybrid spherical material was calcined at 550 °C for 3 hours using a heating rate of 5 °C/min. The surface coating of the silica spheres with titanium was made from the wet impregnation of its organic precursor, where 1.0 mL of titanium isopropoxide (Aldrich) was added to 25 mL of isopropyl alcohol containing 1.0 g of the silica spheres, keeping the contact under constant stirring for 24 hours. After the spheres drying at room temperature for 24 hours, the calcination was again carried out at 500 °C for 3 hours to form the crystalline TiO₂; the sample was named SiO₂@TiO₂.

Characterization of the SiO₂@TiO₂ spheres

The X-ray diffraction (XRD) measurement was performed in the angular range (2θ) of 10–90° with Cu K α , 40 kV and 45 mA. The N₂ adsorption/desorption isotherm was carried out after degassing for 2 hours under vacuum at 200 °C. The scanning electron micrographs, energy dispersive spectroscopy coupled (SEM-EDS) analysis was performed at 10 kV and 2.27 x 10⁻⁷ Pa. Samples were placed in a double-sided carbon tape on aluminium support and metalized with gold in an argon atmosphere at low pressure. The diffuse reflectance spectrum (DRS-UV-vis) was measured in a 300 to 800 nm scanning range.

Photocatalytic Conversion Experiments

The selective photocatalytic conversion reactions of benzyl alcohol to benzaldehyde and nitrobenzene to aniline were performed in a glass reactor with a quartz tube located in the centre using magnetic stirring. A high-pressure mercury lamp (8 W, 315–420 nm, maximum wavelength at 365 nm) was used as an irradiation source. The reaction mixture comprised 0.25 g of SiO₂@TiO₂ spheres with 25 mL of a solution containing the organic compound. For the photocatalytic oxidation reactions, the initial concentration of benzyl alcohol was 10⁻³ mol/L, while in the photocatalytic reduction reactions, the initial concentration of nitrobenzene was 8.0 x 10⁻⁴ mol/L. In both reactions, the solvents were

pre-saturated for 30 minutes with O_2 or N_2 for favouring oxidative or reducing conditions, respectively. The system was kept under magnetic stirring for 1 hour before turning on the lamp to achieve the adsorption equilibrium. The monitoring of composition was done by HPLC using a C18 column (5 μ , Phenomenex) at 210 nm. The mobile phase was composed of methanol, water, and buffer solution in a ratio of 40:20:40 and a flow rate of 1.0 mL/min. The buffer was prepared with 10 mL of H_3PO_4 (5.05 mol/L), 50 mL of methanol, and ultra-pure water, for a total volume of 1 L. To evaluate the isolated effects, TiO_2 powder (P25, Degussa, 0.025 g) and SiO_2 sphere (without titanium dioxide) were tested under the same reaction conditions.

RESULTS

Characterization of the photocatalyst

X-ray diffraction

Figure 1 shows the diffraction profile of the silica spheres (SiO_2) before and after titanium coating ($\text{SiO}_2@\text{TiO}_2$). Both samples show no clear diffraction peak. However, it is observed a broad signal in the 2θ degree range of 15 to 30, which is typical for the SiO_2 samples material heat treated at low temperature (550 °C) (Matos et al. 2011, Pan et al. 2008). Despite that, the diffraction profile for sample $\text{SiO}_2@\text{TiO}_2$ shows a smooth enlargement of the broad signal (emphasized in the inserted figure), which can be attributed to the formation of the tetragonal anatase phase according to the diffraction pattern (ICSD code of 9854) inserted in Figure 1.

In a previous study developed by the authors (Salgado & Valentini 2019), an apparent surface coverage of 13.2% of TiO_2 on the surface of the SiO_2 spheres was estimated through the surface charge (point of zero charge) of SiO_2 , TiO_2 and $\text{SiO}_2@\text{TiO}_2$. The absence of a defined peak demonstrating the presence of TiO_2 can be attributed to the morphological characteristics inherent to the process of

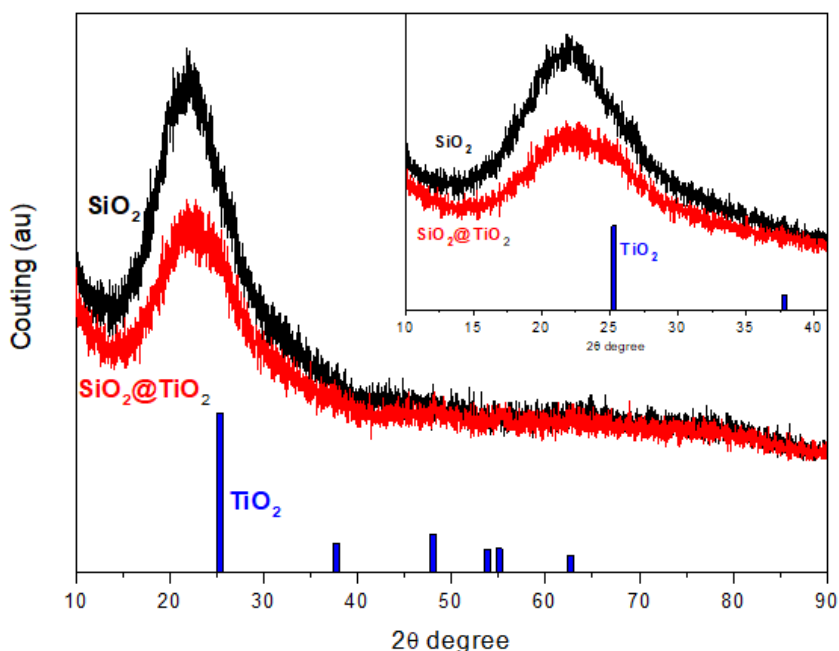


Figure 1. X-ray diffraction profile of the SiO_2 and $\text{SiO}_2@\text{TiO}_2$ spheres.

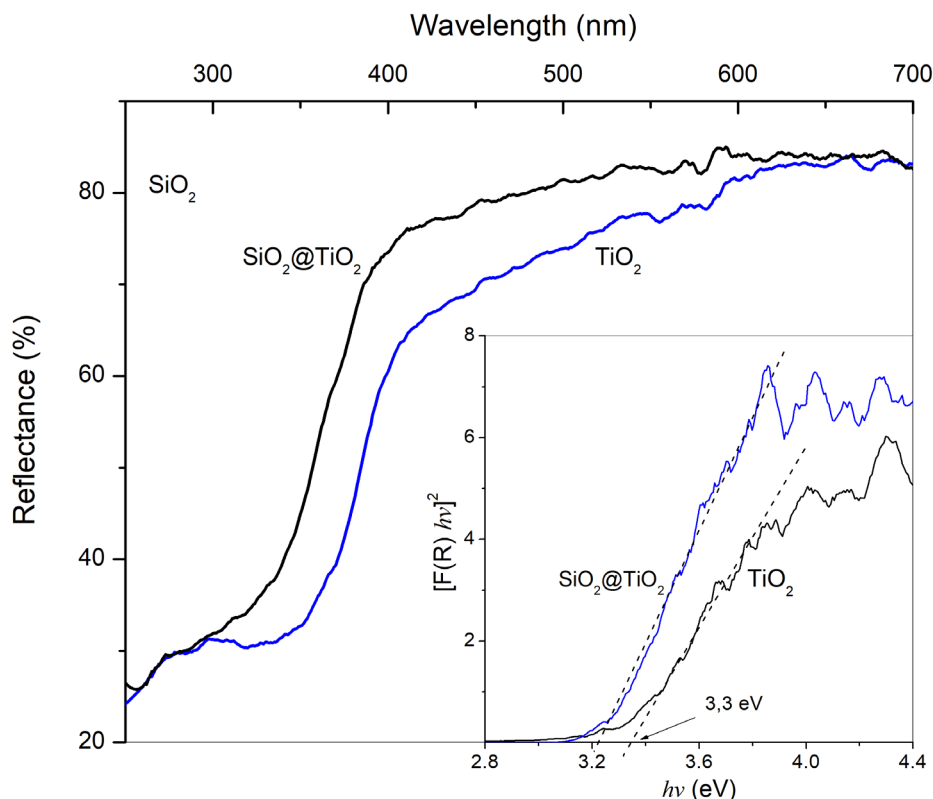


Figure 2. Diffuse reflectance spectrum of SiO₂@TiO₂ spheres, TiO₂ P25 and SiO₂.

synthesis of silica spheres, contributing to a reduced adsorption of the Ti precursor and consequent growth of the TiO₂ particle.

Diffuse reflectance

The optical property of the SiO₂@TiO₂ spheres was determined by diffuse reflectance spectroscopy, as shown in Figure 2. The spheres impregnated with titanium on their surface have an absorption band in the UV region, which is attributed to the charge transfer process of the valence band of the 2p orbital of the O²⁻ ions to the conduction band of the t_{2g} orbitals of the Ti⁴⁺ (Loddo et al. 1999). The bandgap determination of the photocatalyst can be performed by applying the Kubelka-Munk function $[(1-R)/2R]^2$ to the reflectance spectral data of the material. Knowing that the TiO₂ phase has a direct bandgap (Yu et al. 2011), the bandgap value is obtained from the intercept of the graph generated by $[F(R)/hv]^2$ vs. hv . The SiO₂@TiO₂ spheres show 3.33 eV, near the value determined for the P25 (3.22 eV), which is close to the anatase phase of TiO₂ (3.2 eV) (Jaroenworarluck et al. 2012, Mahesh et al. 2015).

Considering the negligible absorption of silica (SiO₂) in the range from 250 to 700 nm, as shown in Figure 2, the behavior presented in the diffuse reflectance spectrum is attributed exclusively to TiO₂. The potentials of the valence (BV) and conduction (BC) bands can be calculated through the Mulliken electronegativity and band-gap of the semiconductor (Cheng et al. 2019), according to equations 1 and 2.

$$E_{VB} = X - E_e + 0.5 E_g \quad (1)$$

$$E_{CB} = E_{VB} - E_g \quad (2)$$

Where E_g , E_{VB} e E_{CB} are the band-gap and potentials of the valence and conduction bands of the semiconductor, respectively, E_e is the energy of free electrons of the hydrogen scale (4.5 eV), and X is the absolute electronegativity (Mulliken) of the atom semiconductor, expressed as the geometric mean of the absolute electronegativity of the constituent atoms, which is defined as the arithmetic mean of the atomic electro affinity and the first ionization energy.

Considering the band-gap of 3.3 eV (Fig. 2) and the X value for TiO₂ of 5.81 eV, the calculated values of E_{VB} and E_{CB} for the SiO₂@TiO₂ spheres were 2.96 and -0.34 eV.

Textural properties and chemical composition

The specific surface area and pore size distribution of the spheres were determined by adsorption/desorption isotherms of N₂ (Figure 3, Table I). The spheres have isothermal profiles typical of types II and III, besides indicating the formation of pores in the form of slits characteristic of the hysteresis of type H3 (Thommes et al. 2015). In both samples, SiO₂ and SiO₂@TiO₂, the pore diameter distribution profile show the presence of micropores (< 2 nm) and mesopores (pores 2–50 nm), but with a predominance of macropores (> 50 nm), as indicated by the isothermal profiles.

The addition of titanium on the silica spheres caused a considerable effect on the surface area, decreasing from 317 to 147 m²/g. Similarly, as points out the pore size distribution (inserted in Figure 3), it is also observed effect over the pore volume, which decreases from 2.402 to 1.191 cm³/g; due to Ti impregnation. However, there was no change in the pore distribution profile. This fact suggests a homogeneous distribution of TiO₂ across the surface of SiO₂, both in the micropores and in the macropores. The SiO₂@TiO₂ spheres were analyzed for morphology and composition by scanning electron microscopy (Figure 4). The synthesized material showed spherical morphology with an average diameter of 1 μm (Figure 4a), which is a pellet diameter easier to recover from the reactional solution.

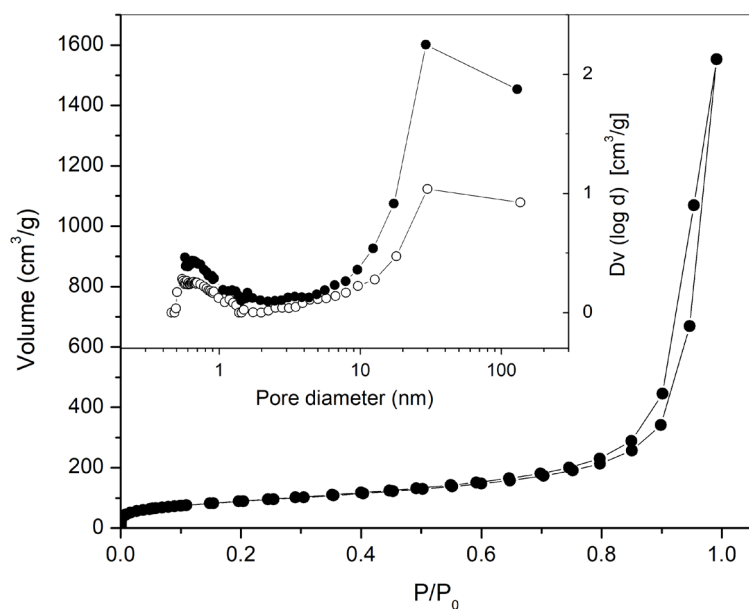


Figure 3. N₂ adsorption/desorption isotherms and pore size distribution (inserted) of the SiO₂ (●) and SiO₂@TiO₂ (○) spheres.

Table I. Specific surface area and pore volume of the spheres from N₂ adsorption/desorption isotherms.

Material	S _{BET} (m ² /g)	V* (cm ³ /g)
SiO ₂	317	2.402
SiO ₂ @TiO ₂	147	1.191

V* – pore volume determined at P/P₀ = 0.995.

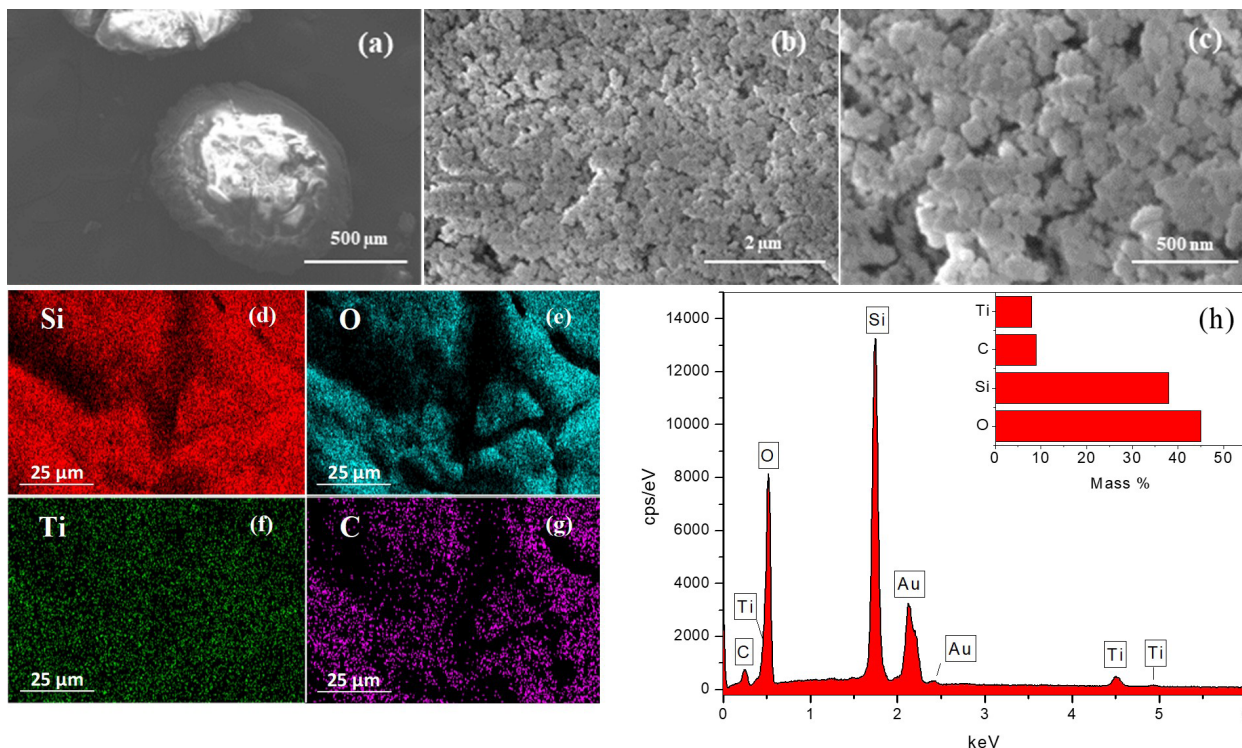


Figure 4. Images of scanning electron microscopy (a-c) and elemental mapping (d-h) of the $\text{SiO}_2@\text{TiO}_2$ spheres. Zoom of 100x (a), 30,000x (b) e 100,000x (c).

Figures 4b-c show the surface sphere morphology, which is composed of interconnecting platelets. This aspect is due to the synthesis route, which uses TEOS and particulate SiO_2 (Aerosil). The TEOS undergoes hydrolysis and then reacts with the SiO_2 particle surface (platelet) at the silanol group, linking the platelets and producing a sample with high pore volume and pore diameter (Table I).

The results of elemental mapping by EDS indicate that the proposed synthesis methodology led to a homogeneous deposition of Ti on the surface of SiO_2 spheres (Figure 4f). The Figures 4g-h show the presence of residual carbon (near 9 wt%), despite the calcination at 550 °C/3h, this is consistent with previous results which shows mass elimination up to 600 °C (Braga et al. 2009), it is important to point out that the second calcination temperature, after the titanium isopropoxide impregnation, the sample was calcined at 500 °C. Considering the platelet condensation, it is reasonable to propose retaining a small fraction of carbon in the pore of the material or between the platelets.

Photocatalytic activity

Photocatalytic oxidation of benzyl alcohol to benzaldehyde

Several authors reported the photocatalytic partial oxidation of alcohols to aldehyde (Augugliaro et al. 2008, Li et al. 2012, Palmisano et al. 2007b; Spasiano et al. 2013, Xie et al. 2014). The reaction is called selective photocatalytic conversion or partial photocatalysis (Augugliaro et al. 2008), which has emerged as a vital field in the photocatalytic area for 'green synthesis' in fine chemistry and efficient

energy conversion since it produces a useful compound (-CHO) instead of its decomposition (CO₂ and H₂O).

The photocatalytic conversion of benzyl alcohol to benzaldehyde is possible due to the higher standard potential of the TiO₂ valence band (2.96 V) compared with the oxidation reaction (Eq. 3) (Xiao et al. 2013):

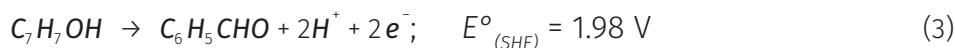


Figure 5 shows the O₂ effect over the conversion of benzyl alcohol to its corresponding aldehyde (benzaldehyde), using acetonitrile as solvent. A test was carried out under the same conditions without catalyst (SiO₂@TiO₂) with the presence of O₂, in which conversion of benzyl alcohol was not observed. The replacement of O₂ with N₂ leads to a decrease in both the conversion rate of benzyl alcohol (48.7% to 22.3%) and the rate of production of benzaldehyde (45.2 to 20.9%) (Figure 5), suggesting that O₂ plays an essential role in the photocatalytic oxidation of benzyl alcohol. This fact is consistent with the fundamental reactions of the photocatalytic process, where the molecular O₂ adsorbed on the surface of the photocatalyst act as an electron acceptor, favouring the separation of the electron/hole pair, leading to the maintenance of the photocatalyst in its excited state. Similar results are reported (Xiao et al. 2013), where a conversion rate of the same order was achieved using a photocatalyst of composition Bi₁₂O₁₇Cl₂ under irradiation in the visible range.

Despite the effect over the benzyl alcohol conversion, the O₂ replacement with N₂ has no impact on the selectivity of the reaction to produce benzaldehyde, reaching levels of 100%.

Figure 6 shows the solvent effect. The replacement of acetonitrile by water under the same reaction conditions shows that the presence of water assumes high relevance in the photocatalytic oxidation of benzyl alcohol. The reaction performed with water presence resulted in a higher conversion of benzyl alcohol, reaching reduction levels of 54.8% in their concentration. However, this conversion did not produce a stoichiometric amount of its corresponding aldehyde, getting

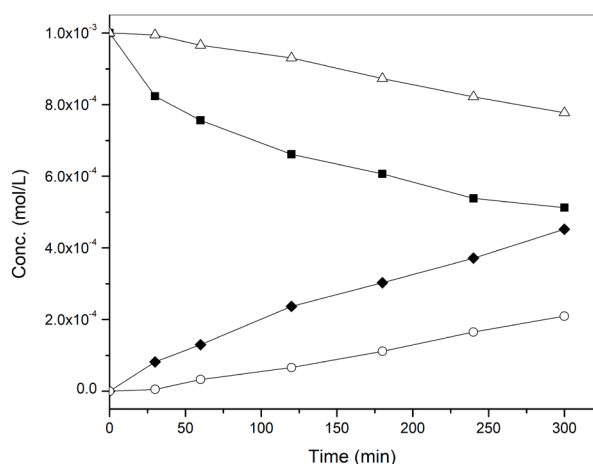


Figure 5. Effect of O₂ in the photocatalytic oxidation of benzyl alcohol. Benzyl alcohol (■ O₂, Δ N₂), benzaldehyde (◆ O₂, ○ N₂). Solvent: ACN. C₀ = 1.0 x 10⁻³ mol/L, SiO₂@TiO₂ = 10 g/L, UV-A (365 nm, 8 W).

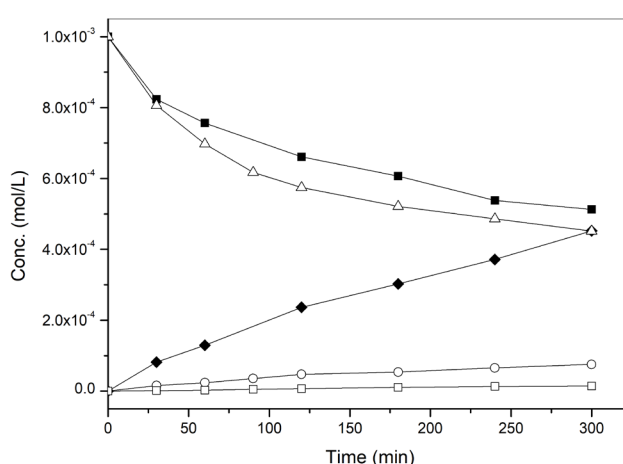


Figure 6. Effect of solvent on the photocatalytic oxidation of benzyl alcohol. Benzyl alcohol (■ ACN, Δ H₂O), benzaldehyde (◆ ACN, ○ H₂O), benzoic acid (□ H₂O). Presence of O₂. SiO₂@TiO₂ = 10 g/L, UV-A (365 nm, 8 W).

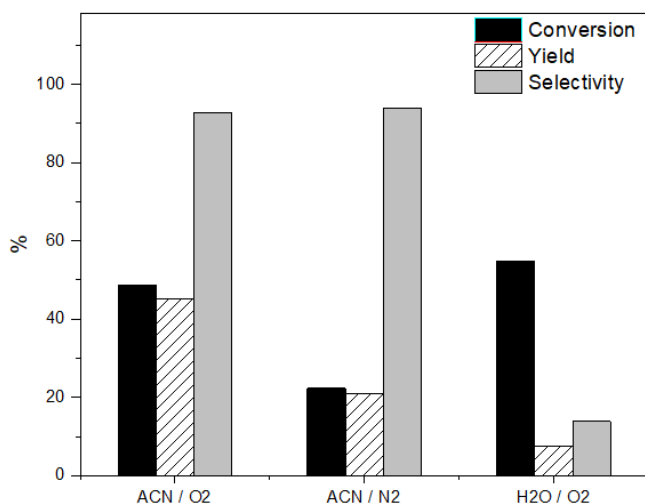


Figure 7. Photocatalytic oxidation of benzyl alcohol to benzaldehyde using SiO₂@TiO₂ spheres under different reaction conditions.

production of only 7.5%. The water presence, which favours the hydroxyl radical formation, produces benzoic acid, pointing out successive reactions and benzyl alcohol decomposition.

Xie et al. (2014) found a similar result, where a photocatalyst composed of In₂S₃ was used in the selective oxidation of benzyl alcohol to benzaldehyde under visible light irradiation in the presence of O₂ in four solvents: trifluorobenzene (TFB), toluene (TOL), acetonitrile (ACN) and water (H₂O). The researchers found a strong effect of the solvent polarity on the reaction performance, where, in terms of production and selectivity, the solvents were ordered as follows: TFB > TOL > ACN > H₂O. The best performance of the photocatalyst in trifluorobenzene was ascribed to a higher solubility of O₂. While the water using as solvent affect the performance of the photocatalyst negatively. This fact is due to the production of highly reactive radical species (OH), which reacts non-selectively with the adsorbed organic substrate. Consequently, the photocatalytic conversion increase but loses in terms of production and selectivity. This finding is strengthened by the production of benzoic acid with water as the solvent, which suggests the occurrence of reactions in series due to the constant non-selective attack of hydroxyl radicals to benzyl alcohol and benzaldehyde.

In reaction condition with O₂ and acetonitrile as the solvent, the silica spheres without titanium did not show photocatalytic activity. At the same time, using TiO₂ powder (P25) led to the conversion of 62% of benzyl alcohol and production of 45% to benzaldehyde. Despite the greater conversion capacity of TiO₂ into powder, the selectivity to benzaldehyde was lower, in addition to the fact that the application in powdered form confers a dispersion of particles that do not sediment under the action of gravity, imposing the need for one more step for recovery of the catalyst.

Figure 7 compares the photocatalytic performance of the SiO₂@TiO₂ spheres in the oxidation of benzyl alcohol to benzaldehyde under different experimental conditions.

A comparative analysis of the data presented in Table II allows concluding that the SiO₂@TiO₂ beads showed photocatalytic efficiency in the oxidation of benzyl alcohol to benzaldehyde, obtaining conversion and selectivity values similar to those reported by other researchers when using acetonitrile as solvent. The performance of the SiO₂@TiO₂ spheres in the photocatalytic oxidation of benzyl alcohol is even more evident when comparing the power of the irradiation source used (8 W), which is much lower than the other works.

Table II. Comparison of conversion and selectivity of photocatalytic oxidation of benzyl alcohol to benzaldehyde in different studies.

Photocatalyst	Reaction condition	C (%)	S (%)	Reference
In ₂ S ₃	C ₀ = 0.033 M Catalyst = 5.3 g/L Xe (300 W) 4 h Solvent: TFB	41	99.8	Xie et al. 2014
	Solvent: CH ₃ CN	40	8.1	
	Solvent: H ₂ O	95	1.1	
TiO ₂ -anatase	C ₀ = 0.067 M Catalyst = 5.3 g/L UV-A (100 W) 4 h Solvent: CH ₃ CN	44	99	Zhang et al. 2009
TiO ₂ /MAGSNC ^a	C ₀ = 1.5 mM; Catalyst = 1.0 g/L; UV-A (125 W) 4 h Solvent: CH ₃ CN	50	90	Colmenares et al. 2016
	Solvent: H ₂ O	5	41	
HP0,5 ^b	C ₀ = 1.0 mM Catalyst = 0.4 g/L UV-A (125 W) 6 h Solvent: H ₂ O	50	28	Augugliaro et al. 2008
Au/CdMoO ₄	C ₀ = 0.062 M Catalyst = 33.3 g/L Xe (300 W) 4 h Solvent: TBF	32	100	Bi et al. 2015
SiO ₂ @TiO ₂	C ₀ = 1.0 mM Catalyst = 10.0 g/L UV-A (8 W) 5 h Solvent: CH ₃ CN (O ₂)	49	92.8	This study
	Solvent: CH ₃ CN (N ₂)	22	94.0	
	Solvent: H ₂ O (O ₂)	55	13.8	

C: conversion. S: selectivity. ^a MAGSNC: nanocomposites of silica-maghemite; ^b HP: home-prepared (TiO₂ anatase).

Taking into account the experimental data obtained and based on studies reported by other researchers (Feng et al. 2011, Xie et al. 2014, Zhang et al. 2009), a reactive scheme is proposed, presented in the following topics and demonstrated in Figure 8:

1. Alcohol molecule adsorbs on the surface of the beads via a deprotonation process, which reacts with the photogenerated hole (h_{VB}^+) to form a carbonic radical via subsequent deprotonation.
2. In the absence of oxygen, carbon radical loses another electron by reacting again with the hole, leading to the formation of benzaldehyde.

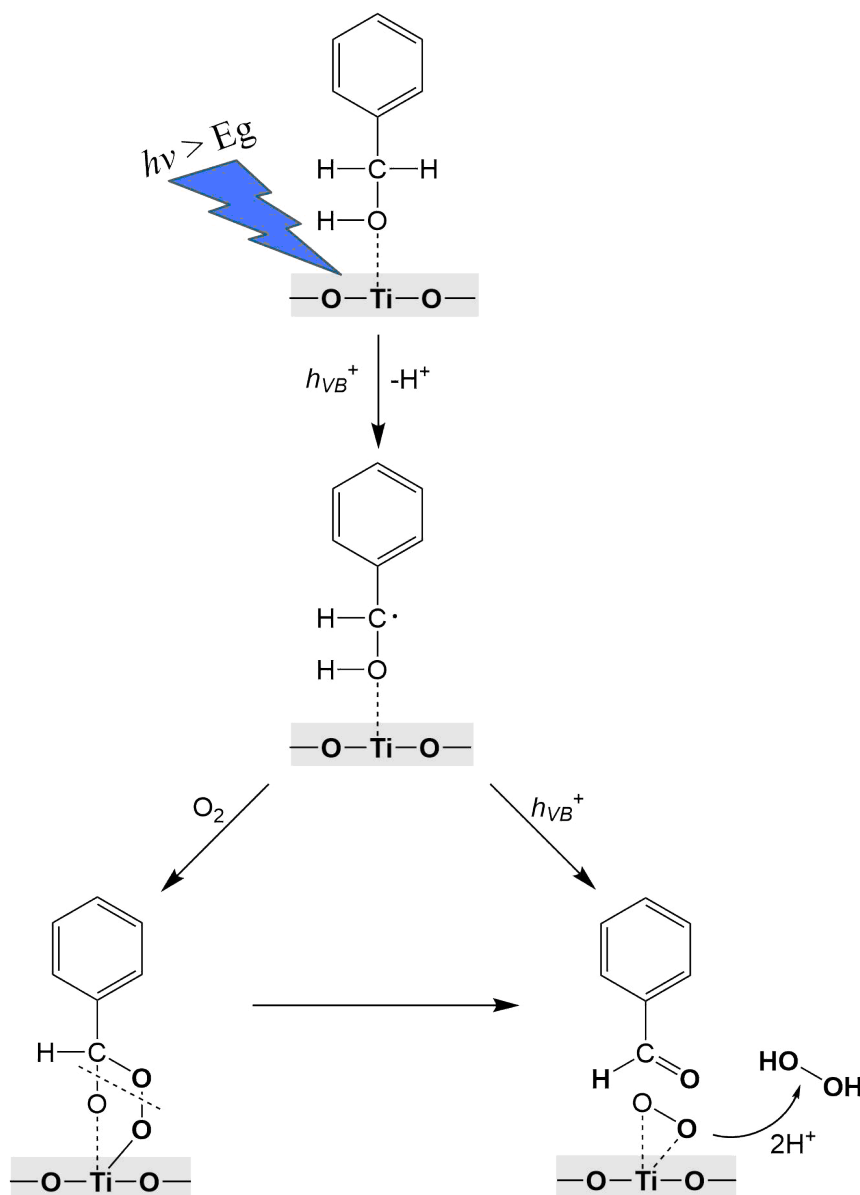


Figure 8. Proposed reaction pathway for selective photocatalytic oxidation of benzyl alcohol to benzaldehyde in the presence of SiO₂@TiO₂ spheres with and without O₂ presence. Adapted from (Feng et al. 2011, Li et al. 2012, Xie et al. 2014, Zhang et al. 2009).

- In the presence of O₂, the superoxide radical formed by the reduction of O₂ in the excited TiO₂ conduction band reacts with the carbon radical, forming an intermediate oxygen bridge structure. The formation of the superoxide radical on the surface of SiO₂@TiO₂ was confirmed in a previous study (Salgado & Valentini 2019) with the use of benzoquinone as a sequestering agent.
- Cleavage of the C-O of the alcohol and O-O of O₂ bonds leads to benzaldehyde formation. The bridged structure of the peroxide bond of TiO₂ can combine with protons to form H₂O₂. In a study performed by Zhang et al. (2009) using oxygen isotopes, it was demonstrated that in the presence of O₂, the O atom of the aldehyde did not originate from the water surface adsorbed or OH groups of TiO₂, but from O₂, indicating an important role of this species when present in the photocatalytic process.

Photocatalytic reduction of nitrobenzene to aniline

The photocatalytic reduction of nitrobenzene to aniline has attracted attention because of the advantages presented in comparison with traditional methods of aniline synthesis, such as room temperature reaction, lower operational costs, and environmental benefits resulting from the significant decrease in waste production (Mohamed & Kadi 2014). In this work, some factors, such as solvent composition and O_2 presence, which affect the performance of the photocatalyst in the reduction reaction of nitrobenzene were evaluated.

Figure 9 shows the O_2 effect over the photocatalytic performance for the reduction of nitrobenzene using methanol as solvent. The presence of O_2 in the medium resulted in a decrease in nitrobenzene conversion levels and aniline production but did not affect selectivity (>99%). The decrease of the reaction rate is due to the competitive effect between nitrobenzene and O_2 by the electrons of the conduction band of the photocatalyst. When adsorbed, O_2 will act as an electron acceptor, with the production of O_2^- radical. Kominami et al. (2009) using TiO_2 presented similar results in the photocatalytic reduction of nitrobenzene in an aqueous medium with the addition of oxalic acid as a hole sequesterant. Additionally, the same authors observed that the O_2 partial pressure increase affects the aniline production.

The effect of the solvent composition was evaluated by carrying out photocatalytic reduction tests of nitrobenzene in methanol or ethanol previously saturated with N_2 (Figure 10).

The reducing reaction of nitrobenzene to aniline shows a meaningful effect of the solvent over the photocatalytic performance. By using methanol, the reaction reached higher conversion levels of nitrobenzene and aniline production if compared with the reaction in ethanol medium. Despite the different performances regarding conversion and production, in both solvents, the selectivity was >99% for aniline and no other product of the reaction was identified. This fact is due to the properties of the solvent, such as viscosity and polarity/polarizability, i.e., the ability of a solvent to stabilize a charge or a dipole through its dielectric constant. An increase in polarity/polarizability corresponds

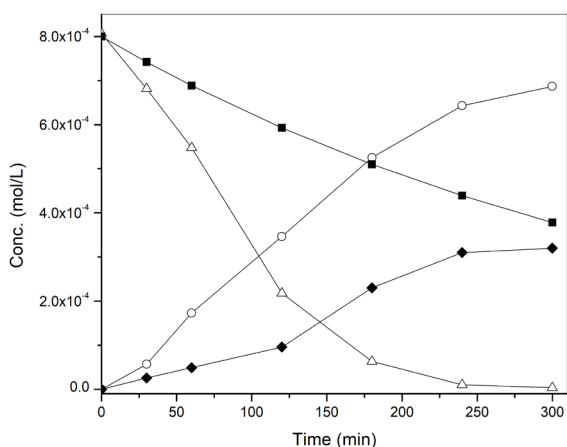


Figure 9. Effect of the presence of O_2 on the photocatalytic reduction of nitrobenzene. Nitrobenzene (\blacksquare O_2 , \triangle N_2), aniline (\blacklozenge O_2 , \circ N_2). Solvent: MeOH. $C_0 = 8.0 \times 10^{-4}$ mol/L, $\text{SiO}_2@\text{TiO}_2 = 10$ g/L, UV-A (365 nm, 8 W).

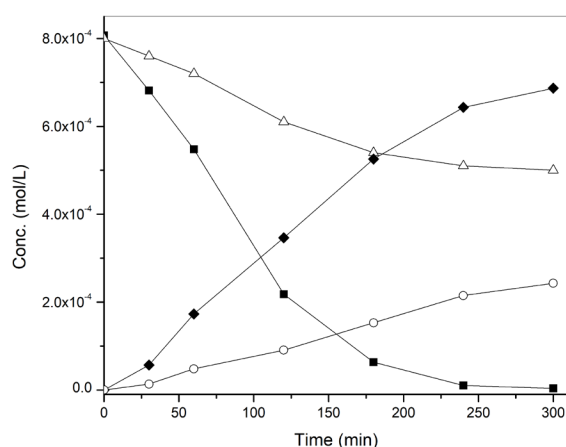


Figure 10. Effect of solvent on the photocatalytic reduction of nitrobenzene. Nitrobenzene (\blacksquare MeOH, \triangle EtOH), aniline (\blacklozenge MeOH, \circ EtOH). $C_0 = 8.0 \times 10^{-4}$ mol/L, $\text{SiO}_2@\text{TiO}_2 = 10$ g/L, UV-A (365 nm, 8 W).

to better stabilization of the charged intermediate species produced, causing an increase in the reaction rate (Palmisano et al. 2007a), which justifies the best performance in methanol medium, given its lower viscosity and higher dielectric constant compared with ethanol. A similar result was reported by Chen et al. (2010) in the photocatalytic reduction of nitrobenzene by TiO₂, where isopropanol was also tested as solvent. These researchers ordered solvents for the performance of the photocatalyst as follows: isopropanol < ethanol < methanol.

On the other hand, it should be considered that the pKa for ethanol (16.0) is higher than methanol (15.5). Therefore, if the proton abstraction from the alcohol is one-step of the process, this short difference between acidity can affect the process.

In addition to alcoholic solvents, the photocatalytic reduction of nitrobenzene was also performed in the aqueous medium. In this condition, no reduction of nitrobenzene concentration was observed, as there was no aniline production. However, the use of acetonitrile promoted a 97% conversion, with a selectivity of 40%. This fact reinforces the effect of the solvent on the development of the photocatalytic process in question. The reduction of nitrobenzene occurs by the electrons present in the conducting band of the photocatalyst, and the photogenerated holes will act in an antagonistic way to the objective of the reaction since they have oxidative properties. As the oxidation potential of the holes present in the valence band is much higher than the reduction potential of the electrons in the conduction band, substances, which are able of inhibiting the action of the holes, must be added. In this sense, methanol will capture photogenerated holes, acting as electron donors, preventing the recombination of the electron/hole pair (Imamura et al. 2013) and inhibiting oxidation reactions.

In reaction condition with N₂ and methanol as solvent, the silica spheres without titanium did not show photocatalytic activity. TiO₂ (P25) powder led to 99% conversion and selectivity of 97.6%.

Table III shows results reported by several authors regarding the application of different photocatalysts in the synthesis of aniline via reduction of nitrobenzene. As shown above, although the reaction time was higher than the other studies, a complete conversion of nitrobenzene to aniline was achieved using a much lower energy source (8 W); for example, when comparing with the work of Huang et al. (2010) where a Xe lamp of 2,000 W was used.

Figure 11 shows a comparative analysis of the performance of the photocatalyst in the different experimental conditions.

Based on the experimental data obtained in this study and on information extracted from studies reported by several researchers (Flores et al. 2007, Jensen et al. 2016, Mohamed & Kadi 2014, Qusti et al. 2014), a reaction mechanism of photocatalytic reduction of nitrobenzene to aniline was proposed, which is detailed in the following topics:

The reaction between methanol and photogenerated hole, producing formaldehyde and H reductor, according to reactions below:



Table III. Conversion and selectivity of the photocatalytic reduction of nitrobenzene to aniline in different studies.

Photocatalyst	Reaction Condition	C (%)	S (%)	Reference
TiO ₂ (MT-150A) R*	C ₀ = 0.01 mol/L Cat. = 10.0 g/L UV-A 400 W, 15 min Solvent: 2-propanol (Ar)	99	98	Imamura et al. 2013
TiO ₂ (JRC-TIO-6) R*		98	97	
TiO ₂ (ST-01) A*		80	75	
TiO ₂ (P25) A, R*		90	83	
TiO ₂ (JRC-TIO-1) A*	C ₀ = 0.01 mol/L Cat. = 1.0 g/L Xe 2,000 W, 4 h Solvent: 2-propanol (N ₂)	21	71	Shiraishi et al. 2012
TiO ₂ (JRC-TIO-2) R*		>99	97	
Ag-TiO ₂	C ₀ = 1.6 × 10 ⁻⁴ mol/L Cat. = 1.0 g/L UV-A 400 W, 1 h Solvent: H ₂ O + CH ₃ OH (N ₂)	86	70	Huang et al. 2010
SiO ₂ @TiO ₂	C ₀ = 8.0 × 10 ⁻⁴ mol/L Cat. = 10.0 g/L UV-A 8 W, 5 h Solvent: CH ₃ OH (N ₂)	>99	85.5	This study
	Solvent: C ₂ H ₅ OH (N ₂)	38	81.0	
	Solvent: CH ₃ OH (O ₂)	53	75.8	

C: conversion. S: selectivity. * TiO₂ supplied from different manufacturers in different phases: anatase (A) and rutile (R).

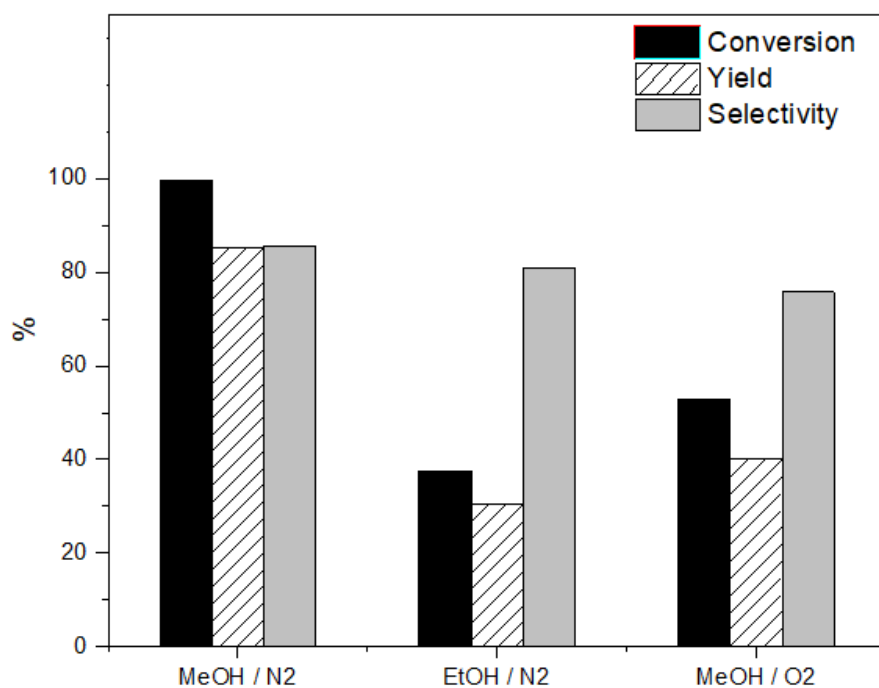
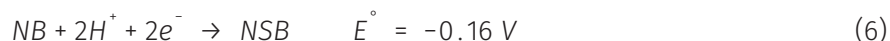


Figure 11. Photocatalytic reduction of nitrobenzene to aniline using SiO₂@TiO₂ spheres under different reaction conditions.

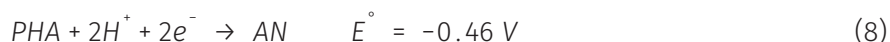
1. The adsorbed nitrobenzene (NB) reacts with the electron of the conduction band and with H⁺, generating the anionic radical NB-N⁻OOH, which gives the intermediate nitrosobenzene (NSB).



2. The NB-N⁻OOH radical is produced from the reduction of the NSB, yielding the intermediate phenylhydroxylamine (PHA).



3. PHA undergoes another electron transfer, producing the radical NB-N⁻OOH, which is easily converted to the aniline (AN). Figure 12 represents the aforementioned topics.



According to Flores et al. (2007) the excess of alcohol solvent used in the experiments and the anaerobic conditions and long periods of irradiation support the hypothesis that the photocatalytic reduction of nitrobenzene occurs mainly by hydroxyalkyl radicals derived from methanol (reaction 3), justifying the occurrence of reaction 8, since the value of the TiO₂ conduction band potential (0.34 V) is not able to lead to the reduction of phenylhydroxylamine to aniline. However, the direct reaction between the electron-accepting substrate (nitrobenzene) and the electrons in the conducting band of the photocatalyst (TiO₂) should also contribute to a significant production of aniline.

Photocatalytic benzyl alcohol oxidation with simultaneously nitrobenzene reduction

The photocatalytic performance study of SiO₂@TiO₂ spheres in simultaneous conversion via oxidation and reduction of benzyl alcohol and nitrobenzene, respectively, was performed in the presence of acetonitrile as a solvent with an initial concentration of 1.0 x 10⁻³ mol/L for both organic compounds. The choice of acetonitrile as a solvent was based on the results presented above. Before lamp activation, the solution was saturated with N₂ to eliminate O₂ and favor nitrobenzene as a species to be reduced by electrons (e_{CB}⁻), and the performance of the material in this condition is shown in Figure 13.

The kinetic profiles presented in Figure 13 show a selective photocatalytic performance to the oxidation of benzyl alcohol over nitrobenzene reduction, showing a decrease in alcohol concentration and proportional production of its respective aldehyde, while for nitrobenzene no change of its concentration was detected and, obviously, without aniline production. As discussed earlier, TiO₂ has a hole (h_{VB}⁺) with much greater potential than the electrons present in the conduction band (e_{CB}⁻), giving the material a predominantly oxidizing characteristic. Besides, the experiment was carried out under identical concentrations of the two substrates with acetonitrile as the solvent, unlike isolated nitrobenzene reduction assays, which occurred under the presence of alcoholic solvents. This fact reinforces the need for a sacrificial agent (alcohol solvent) to inhibit the oxidative activity of the holes and to favor photogenerated electrons to promote reduction reactions with TiO₂.

Figure 14 shows a schematic of the photocatalytic oxidation and reduction reactions of the benzyl alcohol and nitrobenzene, respectively, on the surface of the SiO₂@TiO₂.

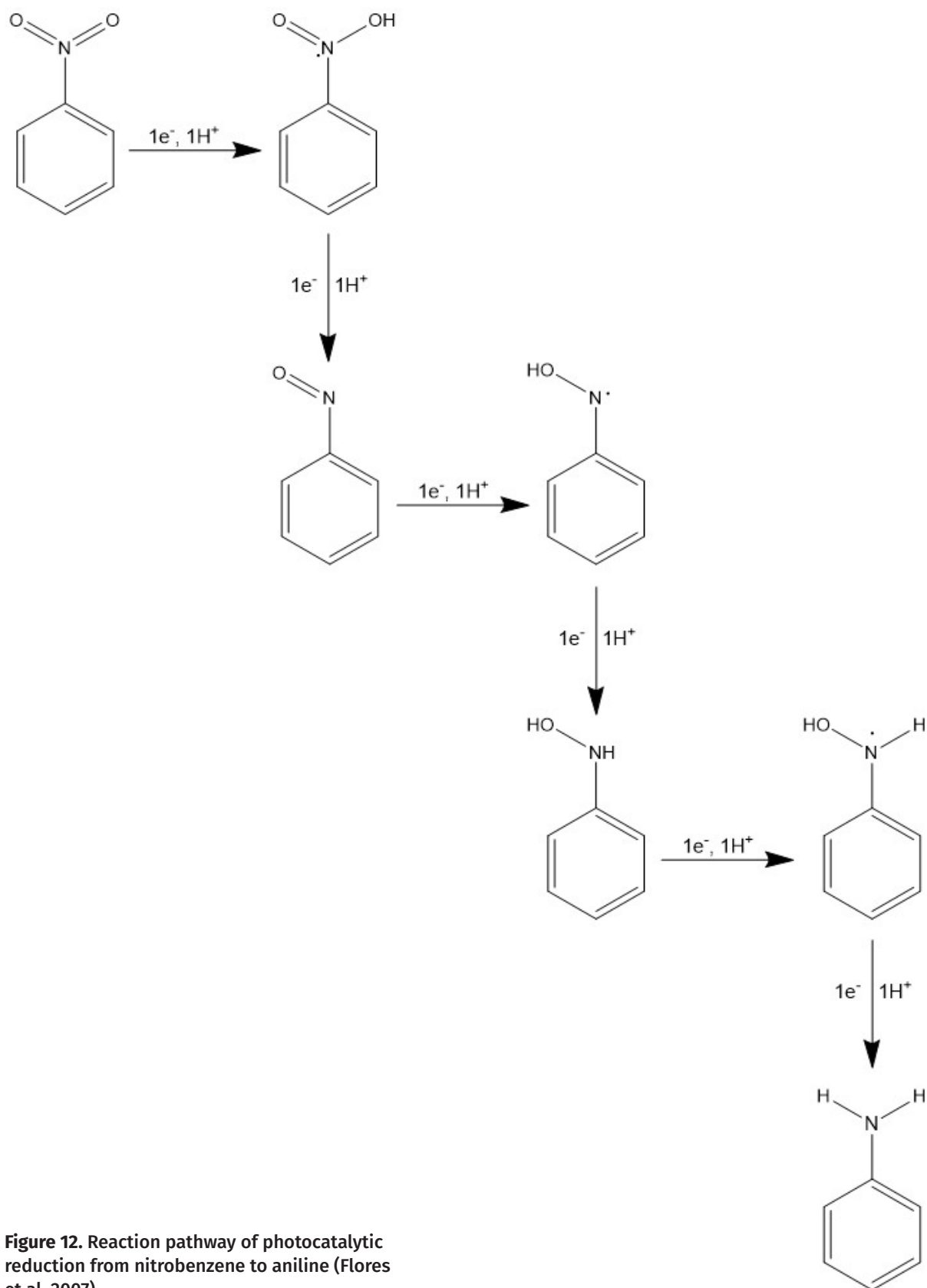


Figure 12. Reaction pathway of photocatalytic reduction from nitrobenzene to aniline (Flores et al. 2007).

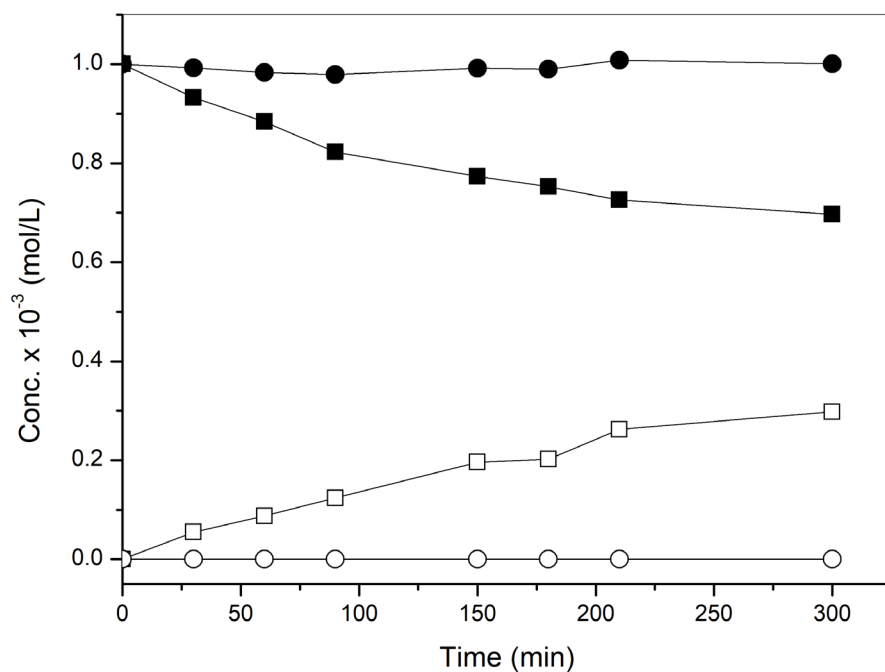


Figure 13. Photocatalytic activity of the $\text{SiO}_2@\text{TiO}_2$ spheres in the simultaneous conversion of BA (■) and NB (●) to BD (□) and AN (○), respectively. $C_0 = 1.0 \times 10^{-3}$ mol/L, $\text{SiO}_2@\text{TiO}_2 = 10$ g/L, UV-A (365 nm, 8 W), solvent: acetonitrile.

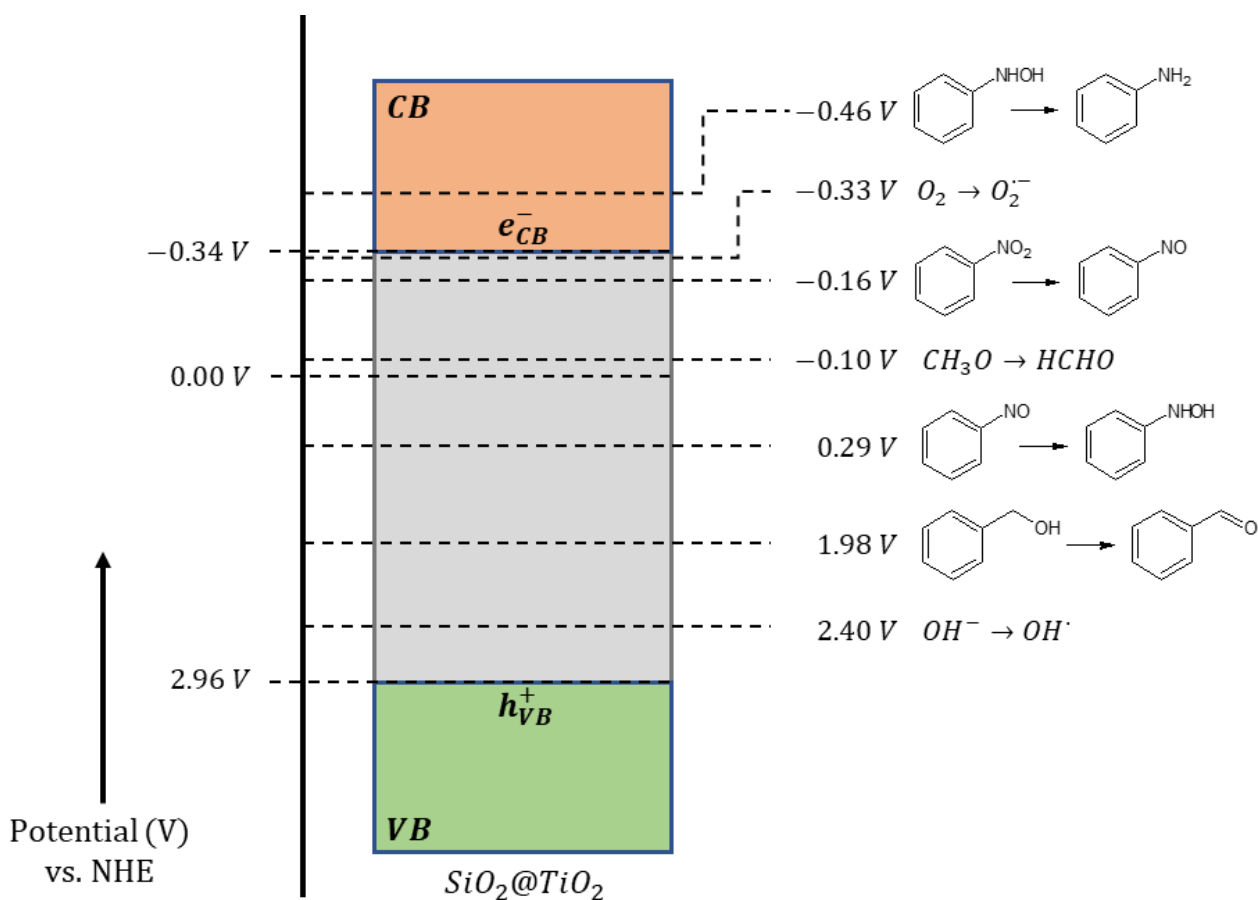


Figure 14. Energy diagram for $\text{SiO}_2@\text{TiO}_2$ and reduction potentials of the main reactions on the surface of the photocatalyst.

CONCLUSIONS

The SiO₂@TiO₂ spheres synthesized presented an amorphous profile with meso and macroporous characteristics. The results indicate a good photocatalytic performance of the spheres concerning the oxidation of benzyl alcohol and reduction of nitrobenzene conversions, with selectivity to benzaldehyde and aniline, respectively. Satisfactory results were obtained with the use of a source of radiation of much lower power than reported for other works. As expected, the presence of O₂ positively affects the oxidation of benzyl alcohol and negatively the reduction of nitrobenzene. The choice of solvent also plays a relevant role, where reactions in the aqueous phase disfavour the selective conversions, requiring organic solvents to achieve better photocatalytic performances. The use of the spheres allows their quick recovery and application in future reactions due to the high sedimentation in contrast to commercially available catalysts.

Acknowledgments

This work was financially supported by the Coordenação de Aperfeiçoamento de Pessoal de Nível Superior (CAPES). We thank the Central Analytical of UFC for SEM-EDX analyses.

REFERENCES

- AFFAM AC & CHAUDHURI M. 2013. Degradation of pesticides chlorpyrifos, cypermethrin and chlorothalonil in aqueous solution by TiO₂ photocatalysis. *J Environ Manage* 130: 160-165. <https://doi.org/10.1016/j.jenvman.2013.08.058>.
- AUGUGLIARO V, KISCH H, LODDO V, LOPEZ-MUÑOZ MJ, MÁRQUEZ-ÁLVAREZ C, PALMISANO G, PALMISANO L, PARRINO F & YURDAKAL S. 2008. Photocatalytic oxidation of aromatic alcohols to aldehydes in aqueous suspension of home-prepared titanium dioxide. 1. Selectivity enhancement by aliphatic alcohols. *Appl Catal A Gen* 349: 182-188. <https://doi.org/10.1016/j.apcata.2008.07.032>.
- BAIH, ZHOU J, ZHANG H & TANG G. 2017. Enhanced adsorbability and photocatalytic activity of TiO₂-graphene composite for polycyclic aromatic hydrocarbons removal in aqueous phase. *Colloids Surfaces B Biointerfaces* 150: 68-77. <https://doi.org/10.1016/j.colsurfb.2016.11.017>.
- BELLARDITA M, ADDAMO M, DI PAOLA A, MARCÌ G, PALMISANO L, CASSAR L & BORSA M. 2010. Photocatalytic activity of TiO₂/SiO₂ systems. *J Hazard Mater* 174: 707-713. <https://doi.org/10.1016/j.jhazmat.2009.09.108>.
- BERBERIDOU C, KITSIOU V, KAZALA E, LAMBROPOULOU DA, KOURAS A, KOSMA CI, ALBANIS TA & POULIOS I. 2017. Study of the decomposition and detoxification of the herbicide bentazon by heterogeneous photocatalysis: Kinetics, intermediates and transformation pathways. *Appl Catal B Environ* 200: 150-163. <https://doi.org/10.1016/j.apcatb.2016.06.068>.
- BI J, ZHOU Z, CHEN M, LIANG S, HE Y, ZHANG Z & WU L. 2015. Plasmonic Au/CdMoO₄ photocatalyst: Influence of surface plasmon resonance for selective photocatalytic oxidation of benzylic alcohol. *Appl Surf Sci* 349: 292-298. <https://doi.org/10.1016/j.apsusc.2015.04.213>.
- BRAGA TP, GOMES ECC, DE SOUSA AF, CARREÑO NLV, LONGHINOTTI E & VALENTINI A. 2009. Synthesis of hybrid mesoporous spheres using the chitosan as template. *J Non Cryst Solids* 355: 860-866. <https://doi.org/10.1016/j.jnoncrysol.2009.04.005>.
- BUCK KT, BOEING AJ & DOLFINI JE. 1987. Method of producing benzaldehyde. *US Pat Off* 4673766.
- CHEN S, ZHANG H, YU X & LIU W. 2010. Photocatalytic Reduction of Nitrobenzene by Titanium Dioxide Powder. *Chin J Chem* 28: 21-26.
- CHENG Y, HE L, XIA G, REN C & WANG Z. 2019. Nanostructured g-C₃N₄/AgI composites assembled by AgI nanoparticles-decorated g-C₃N₄ nanosheets for effective and mild photooxidation reaction. *New J Chem* 43: 14841-14852. <https://doi.org/10.1039/c9nj02725d>.
- COLMENARES JC, OUYANG W, OJEDA M, KUNA E, CHERNYAYEVA O, LISOVYTSKIY D, DE S, LUQUE R & BALU AM. 2016. Mild ultrasound-assisted synthesis of TiO₂ supported on magnetic nanocomposites for selective photo-oxidation of benzyl alcohol. *Appl Catal B Environ* 183: 107-112. <https://doi.org/10.1016/j.apcatb.2015.10.034>.
- COLPINI LMS, LENZI GG, URIO MB, KOCHEPKA DM & ALVES HJ. 2014. Photodiscoloration of textile reactive dyes on Ni/TiO₂ prepared by the impregnation method: Effect of

calcination temperature. *J Environ Chem Eng* 2: 2365-2371. <https://doi.org/10.1016/j.jece.2014.01.007>.

CORMA A, CONCEPCIÓN P & SERNA P. 2007. A different reaction pathway for the reduction of aromatic nitro compounds on gold catalysts. *Angew. Chemie - Int Ed* 46: 7266-7269. <https://doi.org/10.1002/anie.200700823>.

FENG W, WU G, LI L & GUAN N. 2011. Solvent-free selective photocatalytic oxidation of benzyl alcohol over modified TiO₂. *Green Chem* 13: 3265. <https://doi.org/10.1039/c1gc15595d>.

FINČUR NL, KRSTIĆ JB, ŠIBUL FS, ŠOJIĆ DV, DESPOTOVIĆ VN, BANIĆ ND, AGBABA JR & ABRAMOVIĆ BF. 2017. Removal of alprazolam from aqueous solutions by heterogeneous photocatalysis: Influencing factors, intermediates, and products. *Chem Eng J* 307: 1105-1115. <https://doi.org/10.1016/j.cej.2016.09.008>.

FIORENZA R, SCIRÉ S, D'URSO L, COMPAGNINI G, BELLARDITA M & PALMISANO L. 2019. Efficient H₂ production by photocatalytic water splitting under UV or solar light over variously modified TiO₂-based catalysts. *Int J Hydrogen Energy* 44: 14796-14807. <https://doi.org/10.1016/j.ijhydene.2019.04.035>.

FLORES SO, RIOS-BERNIJ O, VALENZUELA MA, CÓRDOVA I, GÓMEZ R & GUTIÉRREZ R. 2007. Photocatalytic reduction of nitrobenzene over titanium dioxide: By-product identification and possible pathways. *Top Catal* 44: 507-511. <https://doi.org/10.1007/s11244-006-0098-2>.

FUKUI M, OMORI Y, KITAGAWA SY, TANAKA A, HASHIMOTO K & KOMINAMI H. 2019. Visible light-induced diastereoselective semihydrogenation of alkynes to cis-alkenes over an organically modified titanium(IV) oxide photocatalyst having a metal co-catalyst. *J Catal* 374: 36-42. <https://doi.org/10.1016/j.jcat.2019.04.022>.

GAO X, GAO K, FU F, LIANG C, LI Q, LIU J, GAO L & ZHU Y. 2020. Synergistic introducing of oxygen vacancies and hybrid of organic semiconductor: Realizing deep structure modulation on Bi₅O₇I for high-efficiency photocatalytic pollutant oxidation. *Appl Catal B Environ* 265: 118562. <https://doi.org/10.1016/j.apcatb.2019.118562>.

GOMES JÚNIOR O, BORGES NETO W, MACHADO AEH, DANIEL D & TROVÓ AG. 2017. Optimization of fipronil degradation by heterogeneous photocatalysis: Identification of transformation products and toxicity assessment. *Water Res* 110: 133-140. <https://doi.org/10.1016/j.watres.2016.12.017>.

GUDE K, GUN'KO VM & BLITZ JP. 2008. Adsorption and photocatalytic decomposition of methylene blue on surface modified silica and silica-titania. *Colloids*

Surfaces A Physicochem Eng Asp 325: 17-20. <https://doi.org/10.1016/j.colsurfa.2008.04.035>.

HO CC, KANG F, CHANG GM, YOU SJ & WANG YF. 2019. Application of recycled lanthanum-doped TiO₂ immobilized on commercial air filter for visible-light photocatalytic degradation of acetone and NO. *Appl Surf Sci* 465: 31-40. <https://doi.org/10.1016/j.apsusc.2018.09.136>.

HORIKOSHI S & SERPONE N. 2020. Can the photocatalyst TiO₂ be incorporated into a wastewater treatment method? Background and prospects. *Catal Today* 340: 334-346. <https://doi.org/10.1016/j.cattod.2018.10.020>.

HUANG H, ZHOU J, LIU H, ZHOU Y & FENG Y. 2010. Selective photoreduction of nitrobenzene to aniline on TiO₂ nanoparticles modified with amino acid. *J Hazard Mater* 178: 994-998. <https://doi.org/10.1016/j.jhazmat.2010.02.037>.

IMAMURA K, YOSHIKAWA T, HASHIMOTO K & KOMINAMI H. 2013. Stoichiometric production of aminobenzenes and ketones by photocatalytic reduction of nitrobenzenes in secondary alcoholic suspension of titanium(IV) oxide under metal-free conditions. *Appl Catal B Environ* 134-135: 193-197. <https://doi.org/10.1016/j.apcatb.2013.01.015>.

ISLAM MT ET AL. 2020. Development of photocatalytic paint based on TiO₂ and photopolymer resin for the degradation of organic pollutants in water. *Sci Total Environ* 704: 135406. <https://doi.org/10.1016/j.scitotenv.2019.135406>.

JAROENWORALUCK A, PIJARN N, KOSACHAN N & STEVENS R. 2012. Nanocomposite TiO₂-SiO₂ gel for UV absorption. *Chem Eng J* 181-182: 45-55. <https://doi.org/10.1016/j.cej.2011.08.028>.

JENSEN SC, HOMAN SB & WEISS EA. 2016. Photocatalytic Conversion of Nitrobenzene to Aniline through Sequential Proton-Coupled One-Electron Transfers from a Cadmium Sulfide Quantum Dot. *J Am Chem Soc* 138: 1591-1600. <https://doi.org/10.1021/jacs.5b11353>.

KOMINAMI H, IWASAKI S, MAEDA T, IMAMURA K, HASHIMOTO K, KERA Y & OHTANI B. 2009. Photocatalytic Reduction of Nitrobenzene to Aniline in an Aqueous Suspension of Titanium(IV) Oxide Particles in the Presence of Oxalic Acid as a Hole Scavenger and Promotive Effect of Dioxygen in the System. *Chem Lett* 38: 410-411. <https://doi.org/10.1246/cl.2009.410>.

KUMARI P, BAHADUR N & DUMÉE LF. 2020. Photo-catalytic membrane reactors for the remediation of persistent organic pollutants – A review. *Sep Purif Technol* 230: 115878. <https://doi.org/10.1016/j.seppur.2019.115878>.

- LAWRENCE FR. 1983. Process for preparing aniline. US4415754A.
- LI CJ, XU GR, ZHANG B & GONG JR. 2012. High selectivity in visible-light-driven partial photocatalytic oxidation of benzyl alcohol into benzaldehyde over single-crystalline rutile TiO₂ nanorods. *Appl Catal B Environ* 115-116: 201-208. <https://doi.org/10.1016/j.apcatb.2011.12.003>.
- LIVINGSTONE K, TENBERGE M, PAPE F, DANILIUC CG, JAMIESON C & GILMOUR R. 2019. Photocatalytic E → Z Isomerization of β-Ionyl Derivatives. *Org Lett* 21: 9677-9680. <https://doi.org/10.1021/acs.orglett.9b03842>.
- LODDO V, MARCÌ G, MARTÍN C, PALMISANO L, RIVES V & SCLAFANI A. 1999. Preparation and characterisation of TiO₂ (anatase) supported on TiO₂ (rutile) catalysts employed for 4-nitrophenol photodegradation in aqueous medium and comparison with TiO₂ (anatase) supported on Al₂O₃. *Appl Catal B Environ* 20: 29-45. [https://doi.org/10.1016/S0926-3373\(98\)00089-7](https://doi.org/10.1016/S0926-3373(98)00089-7).
- MAHESH KPO, KUO DH & HUANG BR. 2015. Facile synthesis of heterostructured Ag-deposited SiO₂@TiO₂ composite spheres with enhanced catalytic activity towards the photodegradation of AB 1 dye. *J Mol Catal A Chem* 396: 290-296. <https://doi.org/10.1016/j.j.molcata.2014.10.017>.
- MARUGÁN J, LÓPEZ-MUÑOZ MJM, VAN GRIEKEN R & AGUADO J. 2007. Photocatalytic Decolorization and Mineralization of Dyes with Nanocrystalline TiO₂/SiO₂ Materials. *Ind Eng Chem Res* 46: 7605-7610. <https://doi.org/10.1021/ie070093u>.
- MATOS J, GARCÍA A & PARK SE. 2011. Ti-containing mesoporous silica for methylene blue photodegradation. *Appl Catal A Gen* 393: 359-366. <https://doi.org/10.1016/j.apcata.2010.12.020>.
- MOHAMED RM & KADI MW. 2014. Green synthesis of aniline by phosphorus-doped titanium dioxide polymorphs. *Ceram Int* 40: 6597-6604. <https://doi.org/10.1016/j.ceramint.2013.11.115>.
- MOLINARI A, SARTI E, MARCHETTI N & PASTI L. 2017. Degradation of emerging concern contaminants in water by heterogeneous photocatalysis with Na₄W₁₀O₃₂. *Appl Catal B Environ* 203: 9-17. <https://doi.org/10.1016/j.apcatb.2016.09.031>.
- MONTEAGUDO JM, DURÁN A, MARTÍN IS & VELLÓN B. 2020. Photocatalytic degradation of aniline by solar/TiO₂ system in the presence of the electron acceptors Na₂S₂O₈ and H₂O₂. *Sep Purif Technol* 238: 116456. <https://doi.org/10.1016/j.seppur.2019.116456>.
- NOSAKA Y & NOSAKA AY. 2017. Generation and Detection of Reactive Oxygen Species in Photocatalysis. *Chem Rev* 117: 11302-11336. <https://doi.org/10.1021/acs.chemrev.7b00161>.
- PALMISANO G, ADDAMO M, AUGUGLIARO V, CARONNA T, GARCÍA-LÓPEZ E, LODDO V & PALMISANO L. 2006. Influence of the substituent on selective photocatalytic oxidation of aromatic compounds in aqueous TiO₂ suspensions. *Chem Commun (Camb)* 9: 1012-1014. <https://doi.org/10.1039/b515853b>.
- PALMISANO G, AUGUGLIARO V, PAGLIARO M & PALMISANO L. 2007a. Photocatalysis: a promising route for 21st century organic chemistry. *Chem Commun* 33: 3425-3437. <https://doi.org/10.1039/b700395c>.
- PALMISANO G, YURDAKAL S, AUGUGLIARO V, LODDO V & PALMISANO L. 2007b. Photocatalytic selective oxidation of 4-methoxybenzyl alcohol to aldehyde in aqueous suspension of home-prepared titanium dioxide catalyst. *Adv Synth Catal* 349: 964-970. <https://doi.org/10.1002/adsc.200600435>.
- PAN YX, LIU CJ & SHI P. 2008. Preparation and characterization of coke resistant Ni/SiO₂ catalyst for carbon dioxide reforming of methane. *J Power Sources* 176: 46-53. <https://doi.org/10.1016/j.jpowsour.2007.10.039>.
- PILLAI UR & SAHLE-DEMESSIE E. 2003. Oxidation of alcohols over Fe³⁺/montmorillonite-K10 using hydrogen peroxide. *Appl Catal A Gen* 245: 103-109. [https://doi.org/10.1016/S0926-860X\(02\)00617-8](https://doi.org/10.1016/S0926-860X(02)00617-8).
- QUSTIAH, MOHAMED RM & ABDELSALAM M. 2014. Photocatalytic synthesis of aniline from nitrobenzene using Ag-reduced graphene oxide nanocomposite. *Ceram Int* 40: 5539-5546. <https://doi.org/10.1016/j.ceramint.2013.10.144>.
- SALAEH S, JURETIC PERISIC D, BIOSIC M, KUSIC H, BABIC S, LAVRENCIC STANGAR U, DIONYSIOU DD & LONCARIC BOZIC A. 2016. Diclofenac removal by simulated solar assisted photocatalysis using TiO₂-based zeolite catalyst; mechanisms, pathways and environmental aspects. *Chem Eng J* 304: 289-302. <https://doi.org/10.1016/j.cej.2016.06.083>.
- SALEHI M, HASHEMIPOUR H & MIRZAEI M. 2012. Experimental Study of Influencing Factors and Kinetics in Catalytic Removal of Methylene Blue with TiO₂ Nanopowder. *Am J Environ Eng* 2: 1-7. <https://doi.org/10.5923/j.aje.20120201.01>.
- SALGADO BCB & VALENTINI A. 2019. Evaluation of the photocatalytic activity of SiO₂@TiO₂ hybrid spheres in the degradation of methylene blue and hydroxylation of benzene: Kinetic and mechanistic

study. *Braz J Chem Eng* 36: 1501-1518. <https://doi.org/10.1590/0104-6632.20190364s20190139>.

SANTOS RCR, PINHEIRO AN, LEITE ER, FREIRE VN, LONGHINOTTI E & VALENTINI A. 2015. Simple synthesis of Al₂O₃ sphere composite from hybrid process with improved thermal stability for catalytic applications. *Mater Chem Phys* 160: 119-130. <https://doi.org/10.1016/j.matchemphys.2015.04.014>.

SERNA-GALVIS EA, SILVA-AGREDO J, GIRALDO AL, FLÓREZ-ACOSTA OA & TORRES-PALMA RA. 2016. Comparative study of the effect of pharmaceutical additives on the elimination of antibiotic activity during the treatment of oxacillin in water by the photo-Fenton, TiO₂-photocatalysis and electrochemical processes. *Sci Total Environ* 541: 1431-1438. <https://doi.org/10.1016/j.scitotenv.2015.10.029>.

SHABAN YA, EL SAYED MA, EL MARADNY AA, AL FARAWATI RK, AL ZOBIDI MI & KHAN SUM. 2016. Photocatalytic removal of polychlorinated biphenyls (PCBs) using carbon-modified titanium oxide nanoparticles. *Appl Surf Sci* 365: 108-113. <https://doi.org/10.1016/j.apsusc.2016.01.001>.

SHIRAISHI Y, TOGAWA Y, TSUKAMOTO D, TANAKA S & HIRAI T. 2012. Highly Efficient and Selective Hydrogenation of Nitroaromatics on Photoactivated Rutile Titanium Dioxide. *ACS Catal* 2: 2475-2481.

SPASIANO D, DEL PILAR PRIETO RODRIGUEZ L, OLLEROS JC, MALATO S, MAROTTA R & ANDREOZZI R. 2013. TiO₂/Cu(II) photocatalytic production of benzaldehyde from benzyl alcohol in solar pilot plant reactor. *Appl Catal B Environ* 136-137: 56-63. <https://doi.org/10.1016/j.apcatb.2013.01.055>.

SPIEGLER L & GRAHAM D. 1958. Hydrogenation of Nitro Compounds to Amines and Catalyst Therefor. *US Pat Off* US2823235A.

TAHIR B & TAHIR M. 2020. Morphological effect of 1D/1D In₂O₃/TiO₂ NRs/NWs heterojunction photo-embedded with Cu-NPs for enhanced photocatalytic H₂ evolution under visible light. *Appl Surf Sci* 506: 145034. <https://doi.org/10.1016/j.apsusc.2019.145034>.

THOMMES M, KANEKO K, NEIMARK AV, OLIVIER JP, RODRIGUEZ-REINOSO F, ROUQUEROL J & SING KSW. 2015. Physisorption of gases, with special reference to the evaluation of surface area and pore size distribution (IUPAC Technical Report). *Pure Appl Chem* 87: 1051-1069. <https://doi.org/10.1515/pac-2014-1117>.

TURCHI C. 1990. Photocatalytic degradation of organic water contaminants: Mechanisms involving hydroxyl radical attack. *J Catal* 122: 178-192. [https://doi.org/10.1016/0021-9517\(90\)90269-P](https://doi.org/10.1016/0021-9517(90)90269-P).

VELA N, MARTÍNEZ-MENCHÓN M, NAVARRO G, PÉREZ-LUCAS G & NAVARRO S. 2012. Removal of polycyclic aromatic hydrocarbons (PAHs) from groundwater by heterogeneous photocatalysis under natural sunlight. *J Photochem Photobiol A Chem* 232: 32-40. <https://doi.org/10.1016/j.jphotochem.2012.02.003>.

WANG D, LIU J, ZHANG M, SONG Y, ZHANG Z & WANG J. 2019. Construction of ternary annular Z-scheme+1Heterojunction CuO/WO₃/CdS/ photocatalytic system for methylene blue degradation with simultaneous hydrogen production. *Appl Surf Sci* 498: 143843. <https://doi.org/10.1016/j.apsusc.2019.143843>.

WANG J, YUAN Z, NIE R, HOU Z & ZHENG X. 2010. Hydrogenation of nitrobenzene to aniline over silica gel supported nickel catalysts. *Ind Eng Chem Res* 49: 4664-4669. <https://doi.org/10.1021/ie1002069>.

WANG R, TANG T, LU G, HUANG K, FENG S, ZHANG X, TAO X, YIN H, LIN Z & DANG Z. 2019. Photocatalytic degradation of polybrominated biphenyls (PBBs) on metal doped TiO₂ nanocomposites in aqueous environments: Mechanisms and solution effects. *Environ Sci Nano* 6: 1111-1120. <https://doi.org/10.1039/c8en01309h>

WOJTYŁA S, ŚPIEWAK K & BARAN T. 2020. Synthesis, characterization and activity of doped graphitic carbon nitride materials towards photocatalytic oxidation of volatile organic pollutants emitted from 3D printer. *J Photochem Photobiol A Chem* 391: 112355. <https://doi.org/10.1016/j.jphotochem.2020.112355>.

XIAO X, JIANG J & ZHANG L. 2013. Selective oxidation of benzyl alcohol into benzaldehyde over semiconductors under visible light : The case of Bi₂O₃/TiO₂ nanobelts. *Appl Catal B Environ* 142-143: 487-493. <https://doi.org/10.1016/j.apcatb.2013.05.047>.

XIE M, DAI X, MENG S, FU X & CHEN S. 2014. Selective oxidation of aromatic alcohols to corresponding aromatic aldehydes using In₂S₃ microsphere catalyst under visible light irradiation. *Chem Eng J* 245: 107-116. <https://doi.org/10.1016/j.cej.2014.02.029>.

YU Q, JIN L & ZHOU C. 2011. Ab initio study of electronic structures and absorption properties of pure and Fe³⁺-doped anatase TiO₂. *Sol Energy Mater Sol Cells* 95: 2322-2326. <https://doi.org/10.1016/j.solmat.2011.03.048>.

ZHANG L, LI P, GONG Z & LI X. 2008. Photocatalytic degradation of polycyclic aromatic hydrocarbons on soil surfaces using TiO₂ under UV light. *J Hazard Mater* 158: 478-484. <https://doi.org/10.1016/j.jhazmat.2008.01.119>.

ZHANG M, WANG Q, CHEN C, ZANG L, MA W & ZHAO J. 2009. Oxygen atom transfer in the photocatalytic oxidation

of alcohols by tio₂: Oxygen isotope studies. *Angew. Chemie Int Ed* 48: 6081-6084. <https://doi.org/10.1002/anie.200900322>.

ZHU X, WANG Y, QIN W, ZHANG S & ZHOU D. 2016. Distribution of free radicals and intermediates during the photodegradation of polychlorinated biphenyls strongly affected by cosolvents and TiO₂ catalyst. *Chemosphere* 144: 628-634. <https://doi.org/10.1016/j.chemosphere.2015.09.039>.

How to cite

SALGADO BCB & VALENTINI A. Photocatalytic performance of SiO₂@TiO₂ spheres in selective conversion of oxidation of benzyl alcohol to benzaldehyde and reduction of nitrobenzene to aniline. *An Acad Bras Cienc* 95: e20220105. DOI: 10.1590/0001-3765202320220105.

*Manuscript received on February 11, 2022;
accepted for publication on May 17, 2022*

BRUNO C.B. SALGADO¹

<https://orcid.org/0000-0002-9858-7836>

ANTONINHO VALENTINI²

<https://orcid.org/0000-0002-7019-6155>

¹Departamento de Química e Meio Ambiente, Instituto Federal do Ceará, Campus Maracanaú, 61939-140 Maracanaú, CE, Brazil

²Departamento de Química Analítica e Físico-Química, Universidade Federal do Ceará, Campus do Pici, 60455-970 Fortaleza, CE, Brazil

Correspondence to: **Bruno C. B. Salgado**

E-mail: brunocesar@ifce.edu.br

Author contributions

Bruno Salgado performed the experimental procedures and analyzed the results. Antoninho Valentini guided the work and contributed to the discussion of the data.

